ELSEVIER

Chemical Geology 191 (2002) 141–154

CHEMICAL GEOLOGY
INCLUDING
ISOTOPE GEOSCIENCE

www.elsevier.com/locate/chemgeo

Transport of uranium, thorium, and lead in metamict zircon under low-temperature hydrothermal conditions

T. Geisler[a,*], R.T. Pidgeon[b], W. van Bronswijk[c], R. Kurtz[a]

[a] *Mineralogisch–Petrographisches Institut der Universität Hamburg, Grindelallee 48, 20146 Hamburg, Germany*
[b] *School of Applied Geology, Curtin University of Technology, GPO Box U 1987, Perth 6845, WA, Australia*
[c] *School of Applied Chemistry, Curtin University of Technology, GPO Box U 1987, Perth 6845, WA, Australia*

Abstract

Understanding the stability of radiation-damaged zircon under low-temperature hydrothermal conditions is crucial to the application of zircon for U–Pb geochronology and as a host phase for the disposal of plutonium waste. We report the results of an investigation of the stability of partially metamict zircon by leaching experiments at 175 °C with a 2 M $AlCl_3$ and a 1 M HCl–$CaCl_2$ solution as hydrothermal fluids for 1340 h. Cathodoluminescence (CL) and backscattered electron (BSE) images show that the zircon grains have developed a reaction rim several micrometers thick or deeply penetrating reticulated alteration zones with sharp boundaries to unaltered metamict zircon. These zones have experienced severe loss of Si, U, Th, and Pb, and gain of Al or Ca, and a water species as revealed by electron microprobe, sensitive high-resolution ion microprobe (SHRIMP) analyses, and infrared spectroscopy. Micro-Raman and infrared measurements on the altered areas show that disordered crystalline remnants of the partially metamict zircon structure were partially recovered, whereas recrystallization of the embedding amorphous phase was not observed. No detectable structural or chemical changes were detected inside the unaltered areas. Intensive fracturing, which was most intense in the HCl–$CaCl_2$ experiment, occurred inside the altered areas due to the volume reduction associated with the recovery of the disordered crystalline material and probably with the leaching reactions. We explain the formation of deep penetrating alteration zones by a percolation-type diffusion model, which is based on the assumption that percolating interfaces or areas of low atomic density between crystalline and amorphous regions as well as between amorphous domains exist along which fast chemical transport is possible. The idea of the existence of fast diffusion interfaces is supported by the sharp chemical gradients at the margin to unreacted zircon. The model was used to estimate for the first time diffusion coefficients for U, Th, and Pb diffusion in amorphous zircon at 175 °C by assuming that volume diffusion inside the amorphous domains is the loss rate-limiting process. These estimates show that volume diffusion in metamict zircon can cause significant loss of U, Th, and especially loss of radiogenic Pb over geological time scales, even at temperatures as low as 175 °C. Our results show that recent Pb loss discordias can be generated (1) by predominate Pb loss from metamict zircon through volume diffusion at low temperatures where thermal healing of the structure is insignificant, and (2) by leaching of Pb (and U and Th) from metamict zircon through an external fluid.
© 2002 Elsevier Science B.V. All rights reserved.

Keywords: Zircon; Leaching; Geochronology; Nuclear waste form

* Corresponding author. Present address: Department of Earth Sciences, University of Cambridge Downing Street, Cambridge CB2 3EQ, UK.

E-mail addresses: tgei01@esc.cam.ac.uk, t.geisler-wierwille@t-online.de, thorsten.geisler@mineralogie.uni-hamburg.de (T. Geisler).

0009-2541/02/$ - see front matter © 2002 Elsevier Science B.V. All rights reserved.
PII: S0009-2541(02)00153-5

1. Introduction

Zircon is a common accessory mineral in a variety of igneous, metamorphic and sedimentary rocks. It is the most commonly used mineral phase in U–Pb geochronology and is a potential host phase for the disposal of weapons-grade plutonium due to its capacity to structurally incorporate actinide ions (Ewing et al., 1995; Ewing, 1999). However, zircon is known to be enigmatic in its resistance to chemical attack. On the one hand, it is known to survive and remain chemically closed under extreme geological conditions (e.g., Ewing, 1999, and references therein) whereas on the other hand, it is also known to lose radiogenic Pb under low P–T conditions, resulting in discordant U–Pb ages (Black, 1987; Hansen and Friderichsen, 1989). In a pioneering study on the stability of the U–Pb system in zircon under hydrothermal conditions, Pidgeon et al. (1966, 1973, 1995) showed that radiogenic Pb could episodically be leached from heavily metamict zircon by sodium chloride solution at temperatures as low as 350 °C. This and subsequent experimental studies have shown that Pb, and under some circumstances U loss from zircon is dependent on the temperature, the nature of the environmental solution, and on the duration of the hydrothermal experiment (Pidgeon et al., 1966, 1973, 1995; Hansen and Friderichsen, 1989; Sinha et al., 1992; Rizvanova et al., 2000; Geisler et al., 2001b). These experiments also verified that self-induced radiation damage of zircon, resulting from the radioactive decay of U and Th (known as metamictization), is an important parameter controlling its resistance to dissolution or selective leaching (Krogh and Davis, 1975; Ewing et al., 1982; Tole, 1985; Sinha et al., 1992; Davis and Krogh, 2000; Rizvanova et al., 2000; Geisler et al., 2001b). However, most of these experiments were made on multigrain samples and results thus represented average effects such that it was impossible to determine Pb and U transport mechanisms in zircon. The major advance in recent experimental studies is the application of micro-imaging and analytical techniques for investigating alteration reactions within single zircon grains. Geisler et al. (2001b) detected sharply bounded, leached, and recrystallized reaction rims around homogenous metamict zircon grains after experimental treatment in a 2 M $CaCl_2$ solution at 450 °C and 1.3 kbar fluid pressure for 1 month. These authors concluded that leaching reactions (including Ca gain and Pb loss) promoted recrystallization, which prevented congruent zircon dissolution and significant U loss. Whereas this model explains high temperature alteration features of natural zircon, the aim of the present investigation was to determine whether it is still valid at temperatures below 200 °C where recovery of metamict zircon may not be activated, even in a hydrothermal environment. A detailed knowledge of the U and Pb transport mechanisms during the fluid–zircon interaction under low-temperature conditions is of great importance for a reliable geological interpretation of discordant U–Pb ages (Stern et al., 1966; Black, 1987). It is also essential for the evaluation of the suitability of zircon as a nuclear waste form because temperatures around 150 to 200 °C are expected to exist in properly designed, deeply buried nuclear waste repositories owing to the geothermal gradients and the excess heat that is produced by radioactive decay (e.g., Brookins, 1984).

2. Methods

2.1. Hydrothermal experiments

We report results from two hydrothermal experiments on a natural zircon from Sri Lanka described below, which were carried out under static conditions with a 2 M $AlCl_3$ solution (run #1t) and a 1 M HCl–$CaCl_2$ solution (run #2t) as the reactive fluid. Whereas ultrapure HCl and $CaCl_2$ were used, it was not possible to commercially purchase $AlCl_3$ with a purity of better than 98%, i.e., the solution contained significant amounts of impurities such as P and Ca. Solutions of extreme pH and/or high salinity were used to enhance possible reactions within laboratory time scales. About 20 grains were placed in Teflon© bombs together with 4 ml of the solution and held at a temperature of 175 °C for 1340 h under autogenous pressure. The temperature was monitored during the experiments to be constant within ± 2 °C.

The choice for Ca- and Al-bearing solutions was suggested by numerous reports of high Ca and Al concentration in natural zircons (e.g., Speer, 1980; Geisler and Schleicher, 2000). Whereas the 2 M $AlCl_3$ solution does not occur in natural environments, we

used this to study the behavior of Al^{3+} during fluid–zircon interaction. The 1 M HCl–$CaCl_2$ solution, however, is closer in composition to natural saline fluids with Ca as the most abundant ion. Ca-rich brines, for example, are known from a number of geological environments such as deeper parts of sedimentary basins (e.g., White, 1965) or crystalline basements (e.g., Frape and Fritz, 1987; Pekdeger et al., 1994). An experimental study has furthermore shown that the boiling of Ca-rich brines produces abundant free HCl in the vapor phase by the hydrolysis of $CaCl_2$, suggesting that considerable amounts of HCl-rich fluids may occur in upper parts of hydrothermal systems (Bischoff et al., 1996).

2.2. Analytical techniques

Quantitative chemical analyses of the run products were carried out with a CAMECA CAMEBAX electron microprobe (EMP) equipped with three spectrometers. The acceleration voltage was 20 kV at ~ 100 nA beam current. Counting times of a single spot analysis with a beam diameter of about 1–2 μm were 10 s for Zr-Lα and Si-Kα, 20 s for Hf-Mα, Y-Lα, P-Kα, Ca-Kα, and Al-Kα, and 60 s for U-Mβ, Th-Mα, Yb-Lα, Er-Lα, and Dy-Lα for the peak and the background. A natural homogeneous zircon chip repeatedly analyzed by SHRIMP was used as standard for U (2454 ± 9 ppm) and Th (810 ± 2 ppm). The background calibration method of Geisler and Schleicher (2000) was used for U and Th analysis. The 2σ counting error for U was ~ 30% at 600 ppm and ~ 7% at 3500 ppm. For Th, we estimated 2σ counting errors between 10% and 50% at concentrations between 800 and 150 ppm.

Sensitive high-resolution ion microprobe (SHRIMP) analyses were made on the WA Consortium SHRIMP II at the Curtin University in Perth, using techniques described by Nelson (1997) and DeLaeter and Kennedy (1998). SHRIMP II uses a primary O_2^- beam focused on a 25–40-μm diameter spot on the target zircon. Analyses were made with a mass resolution of about 5000, which was sufficient to resolve isobaric interference. Determination of the Pb–U ratios of the unknown samples was based on the CZ3 standard and determined using the correlation between ln(Pb/U) and ln(UO/U) (Claoué-Long et al., 1995). The 2σ error of 10 standard measurements made during the analytical session was 2.3%.

Raman spectra were collected with an ISA Lab-Ram dispersive spectrometer using the 632.187-nm line of a NeNe laser and a beam power of 14 mW at the exit of the laser. A 100× objective (N.A. = 0.9) was used, resulting in a lateral spot size of ~ 1 μm. The spectral resolution was 2.5 cm^{-1}. More analytical details are given elsewhere (Geisler et al., 2001b). Raman imaging was carried out with a step size of 1 μm and a counting time of 10 s for each point.

Unpolarized reflectance infrared spectra were recorded with a Bruker Equinox 55 spectrometer in the frequency region between 600 and 6000 cm^{-1}. The measurements were carried out on an A590 microscope by narrowing the beam with a 50-μm aperture. The spectral resolution was 4 cm^{-1}. The large spot size limited the infrared measurements to thick reaction rims as observed in the HCl–$CaCl_2$ experiment (run #2t).

2.3. Starting sample

The starting material consisted of abraded grains of a large natural gem-type, and heavily metamict zircon from Sri Lanka (CZ25). The $^{207}Pb/^{206}Pb$ SHRIMP age of this sample is 524 ± 5 Ma (2σ). Optical investigations of grains used for the experiments did not show any significant zoning although SHRIMP and electron microprobe measurements on different grains of the starting material revealed a slightly heterogeneous elemental distribution. Low Ca (< 45 ppm) and Al (< 30 ppm) concentrations indicate that the sample is virtually unaltered. A complete chemical analysis of the starting material is given in Table 1. SHRIMP analyses of the starting material are compiled in Table 2.

Based on the cumulated α-decay dosage (~ 5.9×10^{18} α-decays/g) and the amorphous fraction versus α-decay dosage calibration for Sri Lanka zircons of Ríos et al. (2000), the sample contains about 15% crystalline remnants located inside an amorphous matrix, i.e., the sample is close to the second percolation point proposed by Salje et al. (1999). Such a microstructure consisting of crystalline remnants in an amorphous matrix has been documented by a number of previous TEM studies on heavily metamict Sri Lankan zircons (Murakami et al., 1991; Weber et

Table 1
Representative electron microprobe data

Label	CZ25[a]	Run #1t				Run #2t			
	Starting material	Rim	Rim	Core	Core	Rim	Rim	Core	Core
ZrO_2	66.5 ± 0.9	68.7	69.0	66.5	65.8	71.8	71.2	66.6	66.8
SiO_2	30.5 ± 0.3	23.2	24.3	30.4	30.8	18.5	19.0	30.4	30.6
HfO_2	1.14 ± 0.07	1.17	1.25	1.15	1.13	1.51	1.33	1.09	1.11
Y_2O_3	0.224 ± 0.063	0.055	0.023	0.227	0.243	0.078	0.053	0.271	0.256
P_2O_5	0.119 ± 0.025	0.384	0.252	0.128	0.109	0.081	0.075	0.050	0.038
CaO	nd	0.271	0.267	nd	nd	1.162	1.482	nd	nd
Al_2O_3	nd	2.496	2.623	nd	nd	nd	nd	nd	nd
ΣREE[b]	0.174 ± 0.080	0.059	0.079	0.219	0.112	0.038	0.039	0.143	0.178
UO_2	0.373 ± 0.045	0.088	0.109	0.383	0.386	0.067	0.065	0.430	0.416
ThO_2	0.084 ± 0.013	0.013	0.033	0.090	0.094	0.025	0.029	0.096	0.091
Total	99.10 ± 0.30	96.51	97.87	99.14	98.72	93.20	93.30	99.03	99.47
H_2O[c]	0.90 ± 0.30	3.49	2.13	0.86	1.28	6.80	6.70	0.97	0.53

nd = Not detected.
[a] Uncertainties represent the empirical 2σ standard deviation of the single measurement around the mean, as estimated from 18 measurements on the starting material.
[b] ΣREE = $Dy_2O_3 + Er_2O_3 + Yb_2O_3$.
[c] Calculated by difference.

al., 1994; McLaren et al., 1994; Capitani et al., 2000). Raman and infrared spectroscopy also confirmed the damaged nature of the starting material (see also Figs. 4 and 5).

3. Results and discussion

3.1. Chemical and structural alteration

Scanning electron microscope backscattered electron (SEM-BSE), cathodoluminescence (SEM-CL), and optical differential interference contrast (DIC) images show that zircon grains treated with the $AlCl_3$ solution developed a reaction rim several micrometers thick that forms sharp boundaries with apparently unaltered zircon (Fig. 1A–C), whereas the $HCl–CaCl_2$ solution caused a deep reticulated alteration pattern (Fig. 1D–E) and a milky-white appearance. The formation of alteration zones or rims clearly demonstrates that metamict zircon dissolves incongruently in low-temperature, acidic solutions under static conditions; an observation that raises doubts on published dissolution rates of metamict zircon, which have been determined from Si or Zr release rates (Ewing et al., 1982; Tole, 1985). This is at first glance surprising since the crosslink density of crystalline zircon is zero (Q^0) and thus zircon is expected to dissolve congruently in acidic solutions by the protonation of the Zr−O bonds and direct transformation of the SiO_4 tetrahedra to silicic acid (Tole, 1985).

X-ray scanning images (Fig. 1C and F) and EMP line scans across the reaction rims (Fig. 2) confirm the formation of sharp chemical gradients to apparently unreacted zircon, where no chemical changes could be detected. Si, U, Th, and P in the case of run #2t as well as the rare earth elements were removed from the altered sites, whereas Ca, Al, and P in the case of run #1t, as well as a water species infiltrated the zircon structure to maintain charge balance (Table 1). SHRIMP measurements show that the altered areas also lost nearly all of their radiogenic Pb, resulting in a shift of the $^{206}Pb–^{238}U$ and $^{207}Pb–^{235}U$ ratios in the direction towards the origin in the Concordia diagram, i.e., to the time of experimental Pb loss (Fig. 3). However, the most remarkable chemical alteration is a severe U and Th loss (Fig. 2; Tables 1 and 2), which contradicts with the observed stability of these species in experiments at higher temperatures (Pidgeon et al., 1966, 1973, 1995; Geisler et al., 2001b). A further interesting finding is that the altered areas are relatively enriched in Zr (Fig. 2) and also Hf (Table 1). This observation

Table 2
SHRIMP U–Th–Pb data[a]

Label		U [ppm]	Th [ppm]	Pb [ppm]	$^{206}Pb/^{238}U$	$\pm 1\sigma$	$^{207}Pb/^{235}U$	$\pm 1\sigma$	$^{206}Pb/^{238}$ U age [Ma]	$\pm 1\sigma$	$^{207}Pb/^{235}$ U age [Ma]	$\pm 1\sigma$
Starting material												
CZ25-1		3342	824	268	0.0823	0.0025	0.653	0.020	509	15	510	12
CZ25-2		2849	534	224	0.0818	0.0025	0.651	0.020	507	15	509	12
CZ25-3		3389	867	282	0.0851	0.0026	0.679	0.021	526	15	526	13
CZ25-4		3252	740	262	0.0829	0.0025	0.667	0.021	514	15	519	13
CZ25-5		2716	633	216	0.0818	0.0025	0.650	0.020	507	15	508	12
CZ25-6		3342	824	268	0.0822	0.0025	0.653	0.020	509	15	510	12
2 M $AlCl_3$ solution experiment												
#1t-1-2	core	3315	716	281	0.0884	0.0016	0.699	0.014	546	10	538	8
#1t-2-3	core	2851	521	231	0.0845	0.0016	0.684	0.013	523	9	529	8
#1t-3-2	core	3357	731	282	0.0867	0.0016	0.699	0.014	536	9	538	8
#1t-3-5	core	3448	783	275	0.0820	0.0015	0.664	0.013	508	9	517	8
#1t-2-1	rim	599	133	11	0.0180	0.0004	0.160	0.011	115	2	150	10
#1t-2-2	rim	810	177	16	0.0198	0.0004	0.169	0.010	127	2	159	8
#1t-3-1	rim	809	217	16	0.0192	0.0004	0.179	0.011	123	2	167	10
#1t-3-4	rim	600	162	12	0.0161	0.0004	0.157	0.019	103	2	148	16
#1t-3-6	rim	649	175	11	0.0174	0.0004	0.166	0.013	111	2	156	11
#1t-3-7	rim	467	123	8	0.0149	0.0004	0.090	0.025	96	2	87	23
1 M HCl–$CaCl_2$ solution experiment												
#2t-1-2	core	3136	647	249	0.0840	0.0015	0.676	0.014	520	9	525	8
#2t-2-2	core	3235	692	272	0.0889	0.0016	0.715	0.014	549	10	547	8
#2t-1-1	rim	1049	162	12	0.0115	0.0002	0.089	0.009	73	1	87	8
#2t-2-1	rim	887	138	9	0.0099	0.0002	0.062	0.012	63	1	61	12
#2t-2-3	rim	503	90	9	0.0169	0.0004	0.095	0.020	108	2	92	19
#2t-2-4	rim	827	132	11	0.0125	0.0003	0.097	0.012	80	2	94	11
#2t-3-1	rim	953	146	10	0.0100	0.0002	0.079	0.009	64	1	77	9
#2t-3-2	rim	836	130	10	0.0125	0.0003	0.108	0.012	80	2	104	11

[a] Common lead was corrected using ^{204}Pb and Broken Hill Pb composition.

is in contradiction with results from high temperature (450 °C) hydrothermal experiments where both Zr and Si were found to be depleted in the reaction rims (Geisler et al., 2001b), but agrees with the recent results from leaching experiments on two natural zircons from Madagascar and Brazil in demineralized water at 96 °C for 1 month (Trocellier and Delmas, 2001). In the latter experiments, the Si release rates were found to be four orders of magnitude higher than the Zr release rates. The relative Zr enrichment is the highest in the HCl–$CaCl_2$ experiment, which indicates strong pH dependence. It can be explained by an exchange of hydrogen with Si^{4+} (i.e., a hydrogrossular-type exchange), which suggests the formation of Zr–OH linkages and which increases the weight fraction of Zr in the altered sites. In fact, hydroxyl groups could be qualitatively detected in the thick reaction rims of run #2t (HCl–$CaCl_2$ solution) by unpolarized reflectance infrared measurements (Fig. 4). A significant infrared signal in the frequency region of O–H stretching vibrations around 3500 cm^{-1} and missing signals in the H–O–H frequency regions at ~1600 and ~5200 cm^{-1} suggest that water in these rims occurs mainly as OH^- (Fig. 4B). The sharpness of this bond indicates that the signal is mainly from O–H stretching vibration inside the crystalline material, but we have to stress that reflectance measurements are significantly less sensitive to water species than transmission experiments. We thus cannot exclude (1) that OH groups occur mainly inside the amorphous regions, which, of course, is very likely, (2) that some molecular water has also

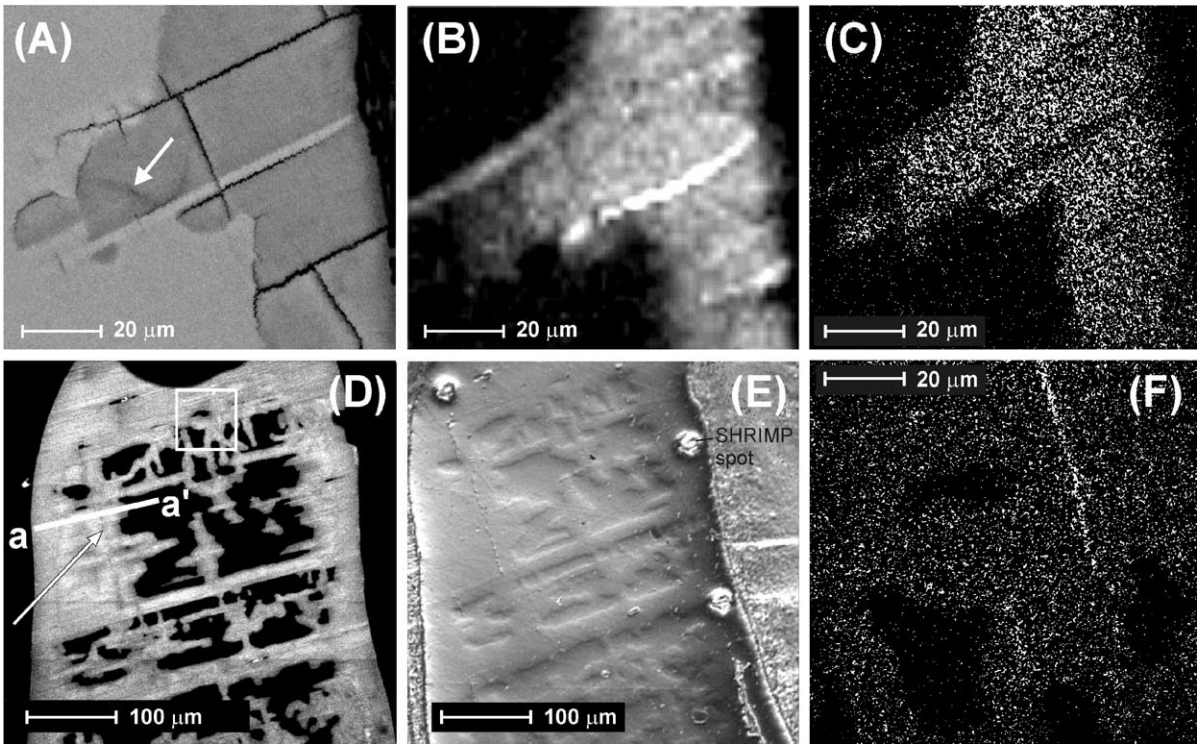

Fig. 1. (A, B, and C) A SEM-BSE image (A), a Raman intensity image of the asymmetrical Si−O band near 1008 cm^{-1} (B), and an Al-Kα X-ray image (C) from the same area of a metamict zircon grain treated with a 2 M $AlCl_3$ solution at 175 °C for 1340 h (run #1t). Note that the grain surface is on the right side of the images. The lower intensity in the SEM-BSE image in (A) reflects a lower mean atomic number of the leached areas due to the infiltration of Al and a water species. Note that the leached and Al-rich area shows a higher Raman intensity, indicating that leaching caused structural recovery (see Fig. 5). White arrow in (A) points to a sealed fracture whereas black fractures in (A) most probably formed during sample preparation. This effect, however, was promoted by internal strain that was most likely caused by the structural recovery and leaching reactions. (D, E, and F) A SEM-CL (D) and a DIC image (E) of the same area of a metamict zircon grain treated with a 1 M HCl–$CaCl_2$ solution at 175 °C for 1340 h (run #2t) while (F) shows a Ca-Kα X-ray scanning image of an area marked in (D) by a white rectangle. We interpret the network-like alteration pattern to be the result of intensive fracturing. The Ca-rich solution could penetrate along the fractures deep into the interior of the grain and from here, an ion exchange front moved into the metamict structure (see Fig. 2B), resulting in a reticulated alteration pattern. White arrow in (D) marks a fracture that runs perpendicular to the EMP profile (a–a′) in Fig. 2B. SHRIMP spots are visible in (E). Some of these fractures, which were resealed during the experiment, are strongly enriched with Ca (see white stripe in (F)).

entered the network and (3) that H_2O was formed by a condensation reaction of the type $Zr(OH)_4 \rightarrow ZrO_2 + 2H_2O$. The latter reaction produces baddeleyite, which cannot be detected by reflectance infrared spectroscopy. Raman spectra from reaction rims of grains treated with the $AlCl_3$ solution do not show any additional bands that can be assigned to ZrO_2. However, we currently cannot completely rule out that a small quantity of baddeleyite was formed during the experiment. Baddeleyite has been observed as a reaction product in hydrothermal experiments on crystalline and metamict zircon with sodium carbonate solution at temperatures as low as 400° (Rizvanova et al., 2000), but has to our knowledge never been reported as a low-temperature hydrothermal alteration product of natural zircon. It is important to emphasize that although the strength of the chemical exchange reaction is different in the two experiments, the loss of trace elements is the same within the experimental error (Fig. 2). Further investigations are underway using various spectroscopic techniques to clarify the nature of the leaching reactions in the amorphous and crystalline regions under various pH and temperature conditions.

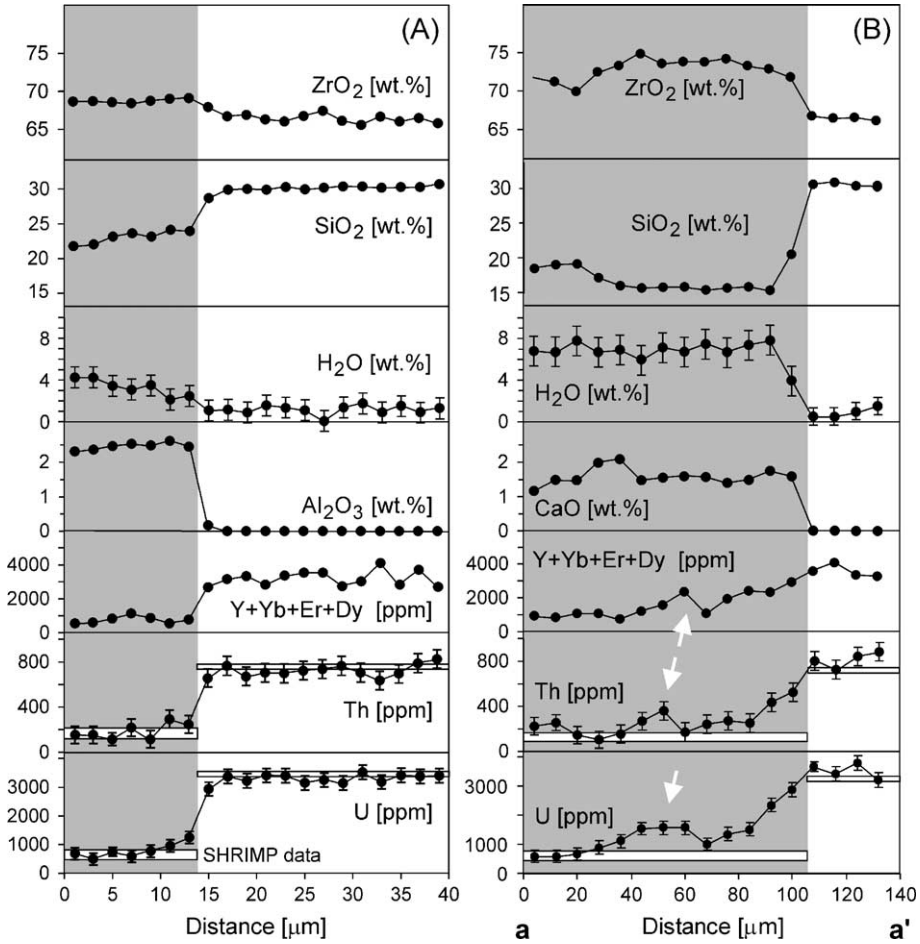

Fig. 2. EMP line profiles across alteration zones (shaded area) into unreacted areas of zircon grains treated with (A) a 2 M $AlCl_3$ solution (run #1t) and (B) a 1 M HCl–$CaCl_2$ solution at 175 °C for 1340 h (run #2t). Note that a comparison with the chemical composition of the starting material shows that the chemistry of the core areas was not altered. The ranges of U and Th concentrations of altered and unaltered areas as determined by SHRIMP measurements on the same grain are shown by white bars for comparison. Note the good agreement between both techniques. The location of profile in (B), a–a′, is marked in (E). The "hills" (white arrows) in the composition profiles in (B) can be explained by the fact that a fracture, running perpendicular to the profile at 70 μm, gave fluid access to deeper parts early in the experiment, resulting in two reaction fronts that were grown together. Error bars are given at the 2σ level.

Micro-Raman measurements clearly show that the structure of the alteration rims around grains treated with $AlCl_3$ solution (run #1t) was partially recovered, as monitored by an increase of the phonon frequency of the asymmetrical Si—O stretching bond and the decrease of its width (Fig. 5). Structural recovery of the altered areas is also clearly indicated by an increased intensity of this band, as shown in two-dimensional Raman intensity images (Fig. 1B). A comparison with results from an isothermal annealing study in air with a similar partially metamict zircon (Geisler et al., 2001a) indicates that the structural transformation process inside the alteration rims only involves the recombination of point defects in the disordered crystalline regions (Fig. 5). From Fig. 5, it is clearly evident that the second recovery stage, which involves epitaxial recrystallization of amorphous zircon, was not reached. The still large line width (~ 24–29 cm^{-1}) of the asymmetrical Si—O stretching band

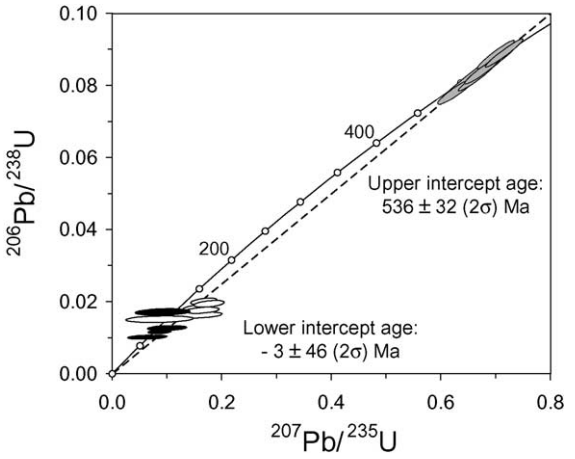

Fig. 3. Concordia plot of SHRIMP analyses of the starting material, unreacted cores (), and of reaction rims of grains treated with a 2 M $AlCl_3$ (run #1t:) and with a 1 M HCl–$CaCl_2$ solution (run #2t:) at 175 °C for 1340 h. The error ellipses define the 2σ analytical uncertainty. Note that the best-fit line (stippled line) extrapolates to the time of the experiment, indicating that Pb isotopes were not significantly fractionated.

can be interpreted to be the result of the confinement of phonons to the small volume of the crystalline remnants, resulting in a fast decay of the phonons and thus in inhomogeneous line broadening (Geisler et al., 2001a). Significant recrystallization of amorphous zircon, however, was observed in reaction rims around grains from a similar metamict zircon treated with a 2 M $CaCl_2$ solution for 1 month at 450 °C (crosses in Fig. 5; Geisler et al., 2001b). It was impossible to get an acceptable Raman spectrum from altered areas of grains from the HCl–$CaCl_2$ experiment due to a severe fluorescence background, which most likely is caused by the high water content in the altered structure (see Fig. 2). Structural recovery of these areas, however, is clearly indicated (1) by reflectance infrared spectra showing an increased reflectivity (Fig. 4A), (2) the increased CL intensity (Fig. 1D, Geisler and Pidgeon, 2001) as well as (3) by an increased hardness as indicated by the topographic differences seen in the DIC images (Fig. 1E).

A further crucial observation for the durability of metamict zircon is the formation of fractures, which provided direct fluid access to the interior of the grains (Fig. 1). This is readily visible in the SEM-BSE image of a grain treated with the $AlCl_3$ solution (run #1t) and shown in Fig. 1A. Here, two types of fractures can be distinguished: one type of fractures, which were resealed during the experiment, allowed solutions to penetrate deeper into the grains, resulting in a tongue-like alteration zones. The unsealed fractures seen in Fig. 1A were most probably caused by the sample preparation (grinding and polishing), but remarkably occur mainly within the reaction rims, indicating that the formation of these fractures is also related to the alteration process. It appears that the formation of fractures in grains treated with the HCl–$CaCl_2$ solution (run #2t) occurred preferentially along cleavage planes, resulting in a network-like alteration pattern (Fig. 1D, E). Accordingly, the 'hills' in the diffusion profiles for U, Th and the REE from this experiment (Fig. 2B) can be explained by the collision of two reaction fronts. One front moved directly from the surface towards the interior of the grain and the other spread out from a fracture that runs parallel to the surface further inside the grain. Fracturing in both experiments was most likely promoted by internal

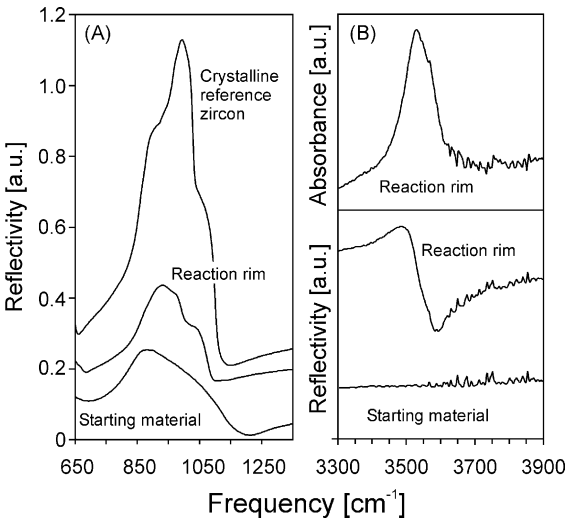

Fig. 4. An unpolarized infrared reflectance spectrum from an altered area of a grain (see Fig. 1D) treated with a 1 M HCl–$CaCl_2$ solution (run #2t) in comparison with those obtained from the starting material in the frequency region between (A) 650 and 1300 cm^{-1} and (B) 3300–3900 cm^{-1}. A spectrum from a crystalline reference zircon is shown in (A) for comparison. The absorption spectrum in (B) was calculated by the Kramers–Kronig transformation from the whole measured spectral range.

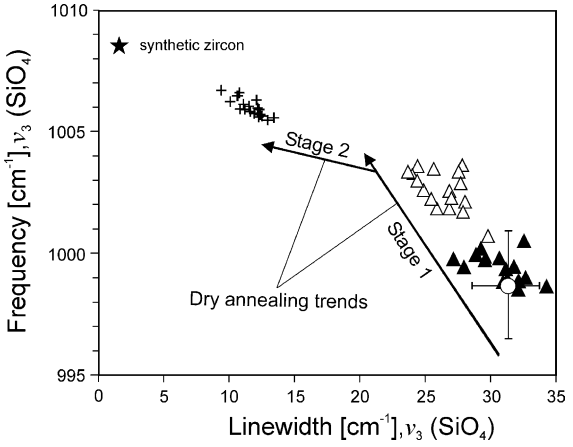

Fig. 5. Variation of the Raman frequency shift of the asymmetrical Si−O stretching bond as a function of its linewidth (expressed as full width at half maximum) of the starting material (○), of unreacted cores (▲), and leached areas (△) of grains treated with a 2 M $AlCl_3$ (run #1t). The shift to higher frequency clearly indicates that structural recovery occurred. Data for reaction rims around a zircon treated at 450 °C in a 2 M $CaCl_2$ solution for 1 month (+) (Geisler et al., 2001b) and for a synthetic crystalline reference zircon are shown for comparison. Solid arrows mark trends obtained by isothermal annealing of a similar partially metamict zircon in a dry ambient under different temperatures (Geisler et al., 2001a). The arrows point to the direction of increasing annealing time. The two linear segments indicate a two-stage annealing process. Stage 1 is dominated by the recovery of the short-range order, i.e., by the recombination of point defects in the crystalline remnants. This stage is followed by the growth of the crystalline domains at the expense of the amorphous material at higher temperatures (Stage 2) (Geisler et al., 2001a). Note that data from the reaction rims from the low temperature experiment (this study) do not reach the second recovery stage, indicating that significant recrystallisation did not occur.

strain due to the volume reduction through the recovery of disordered crystalline domains and probably through the intensive leaching reactions. It is noteworthy that the pattern of experimentally induced fractures, running nearly perpendicular to the reaction front as seen in the $AlCl_3$ experiment, resembles those from natural zircons (Lee and Tromp, 1995). This suggests that the formation of fractures in natural zircon is not necessarily the result of differential expansion of zoned zircon with progressive metamictization (Chakoumakos et al., 1987; Lee and Tromp, 1995), but may also be caused by differential shrinking as a result of structural recovery due to a hydrothermal imprint.

3.2. A model for the transport of U, Th, and Pb in metamict zircon

The fact that no recrystallization of the amorphous phase occurred during the experiments implies that the amount of amorphous and crystalline domains remained unchanged during the experiments and that the alteration process cannot be explained by a dissolution -re-precipitation model. This observation is of great significance as it is the key to understanding the severe loss of U and Th at low temperatures, and opens for the first time perspectives to estimate volume diffusion coefficients for U, Th, and Pb transport in amorphous zircon, which is important for the evaluation of the long-term stability of an actinide-doped zircon waste form. Since experimental studies have shown that volume diffusion of chemical species in crystalline zircon is extremely slow at the temperature used in the experiment (Cherniak et al., 1991, 1997a,b; Lee et al., 1997; ; Cherniak and Watson, 2001), it is most likely that the observed loss of U, Th, and Pb from the leached areas can be attributed entirely to loss from the amorphous phase. However, it is difficult to explain the deep penetrating diffusion front observed within the short time scale of the experiment in terms of uniform diffusion through the bulk amorphous phase, even when considering diffusion through amorphous materials, which is usually faster by several orders of magnitude compared to diffusion through the crystalline counterpart (Petit et al., 1989).

In order to understand this phenomenon, we have to consider the microstructure of partially metamict zircon. The crystalline-to-amorphous transformation in zircon has recently been described (Salje et al., 1999) and modeled (Trachenko et al., 2000) in terms of a percolation-type transition. According to this model, amorphous domains occur as isolated islands within a crystalline matrix at low degree of radiation damage when the system is below the first percolation point. At this stage, diffusion of any particle through the structure at a given temperature is mainly controlled by volume diffusion through crystalline domains. The situation changes above the first percolation point when both amorphous and crystalline domains are interconnected and percolating clusters exist. We propose that in this regime percolating interfaces between crystalline and the amorphous domains provide new high diffusivity pathways. Recent molecular dynamic

simulations (Trachenko et al., 2001; Crocombette and Ghaleb, 2001) and nuclear magnetic resonance studies (Farnan and Salje, 2001) have shown that with increasing degree of amorphization, the amorphous material is polymerized to some extent (an average Q^2 speciation), resulting in a densification of the amorphous domains. This observation contrasts with the finding that with increasing amorphization, the volume swelling of the amorphous material continuously increases (Ríos et al., 2000), implying that structural cavities or areas of low atomic density have to exist (Ríos, in preparation). Such low-density areas could mark the boundaries between amorphous domains and crystalline areas and could, in addition, provide fast diffusion pathways. The existence of fast diffusion pathways is clearly indicated by the relative sharp chemical gradient at the margin to unreacted zircon, which shows that chemical transport through the thick leached area is obviously not rate-limiting. Although we are not yet able to propose a detailed model about the structural state of the amorphous material and the leaching reactions, one might speculate that bond breaking reactions, ion exchange, as well as the release of Si, occur along the surface of such boundary regions, which further opens up these regions with increasing duration of the experiment. It is important to mention that interfaces located between amorphous domains should still percolate above the second percolation point where the connectivity of the interfaces between crystalline and amorphous domains is disrupted. Indeed, recent hydrothermal experiments have demonstrated that after the first percolation point, the ion conductivity continuously increases with the degree of metamictization (Geisler et al., 2001b).

Let us now discuss the implication of this model particularly for the transport of U, Th, and Pb through the metamict network. Before a U, Th or Pb atom can diffuse out of the grain along percolating interfacial regions, it has to leave the amorphous or crystalline domains through volume diffusion. At the margin of a grain, the interface paths or cavities become rapidly saturated with inwards diffusing species, which causes a diffusion-driven chemical gradient between amorphous domains and the interface. It is reasonable to assume (1) that the time an outward diffusing atom spent at the interface is much shorter than the time it required to diffuse out of a crystalline or amorphous domain (i.e., volume diffusion inside the domains is the rate-limiting process), and (2) that the fraction of outwards diffusing atoms in the interface paths after the experiments was insignificant. Assuming further that the average spherical radius, r, of amorphous domains is ≈ 25 Å (e.g., Weber et al., 1994; Ríos et al., 2000), it is possible to estimate the diffusion coefficient for U and Th diffusion in amorphous zircon, D_v^a, from the volume diffusion approximation given by Reichenberg (1953):

$$D_v^a/r^2 = \frac{1}{t}\left[\frac{2}{\pi} - \frac{2}{\pi}\left(1 - \frac{\pi}{3}F\right)^{1/2} - \frac{1}{3}F\right] \quad \text{for } F \leq 0.85$$

$$D_v^a/r^2 = -\frac{1}{\pi^2 t}\ln\left[\frac{\pi^2}{6}(1-F)\right] \quad \text{for } F > 0.85 \qquad (1)$$

where t is the duration of the experiments and F is the fraction of U, Th or any other species lost from amorphous domains. The loss fraction F is given by $F = f/f_a$ where f is the fraction of U and Th loss from the zircon, and f_a the fraction of amorphous domains. The U and Th loss fraction f was calculated from a number of EMP line scans such as those shown in Fig. 2. We used the first three EMP measurements within leached areas and all measurements within the unaltered part of the line scan for the calculation of F. The fraction of amorphous domains, f_a, in the area of each line profile was estimated from the α-decay dose, D, obtained from the U and Th contents of unaltered areas and the dose-dependence of the amorphous fraction for Sri Lanka zircons, as given by the direct impact model $f_a = 1 - e^{-B_a D}$ with $B_a = 2.7 \times 10^{-19}$ g (Ríos et al., 2000). This direct impact relationship has recently been verified by infrared and nuclear magnetic resonance investigations (Zhang and Salje, 2001; Farnan and Salje, 2001) and agrees also with the results of atomistic simulations (Trachenko et al., 2001; Crocombette and Ghaleb, 2001), although future studies should include an incubation dose to account for self-annealing during cooling. However, this would not significantly affect the calculated amorphous fraction for sample CZ25 and thus the conclusion drawn in this paper. Although the SHRIMP age of our sample CZ25 is 524 Ma, we estimated the α-decay dose for an age of 570 Ma to be

consistent with Ríos et al. (2000). Since we did not find any significant differences in the U, Th, and Pb loss between single grains from both experiments (see Fig. 2), F was calculated from the results of both experiments.

With $t = 4.824 \times 10^6$ s, $F = 0.93$ for U, and $F = 0.86$ for Th, we obtain a diffusion coefficient for U and Th diffusion in the amorphous phase of $(2.9 \pm 0.8) \times 10^{-21}$ cm^2 s^{-1} and $(1.9 \pm 0.6) \times 10^{-21}$ cm^2 s^{-1} at 175 °C, respectively. The given errors take into account only the 2σ uncertainty of the U and Th concentrations, i.e., the absolute error of these estimates depend on our model assumptions and is certainly much higher. We carried out the same calculation for Pb by using our SHRIMP analyses from the altered rims and from unaltered sites. We estimated the Pb loss fraction from leached areas in both experiments to be 0.96. Since the average amorphous fraction in our sample is 0.85, Pb was obviously also lost from crystalline domains. The diffusion coefficient for Pb diffusion in amorphous zircon at 175 °C is thus larger than 4×10^{-21} cm^2 s^{-1}, as estimated from Eq. (1) by setting $F = 0.96$ as a lower limit of Pb loss and t and a as given above. As expected, the estimated Pb diffusion coefficient is significantly larger than the previous measured diffusion coefficients in crystalline zircon extrapolated to 175 °C (Bogomolov, 1991; Lee et al., 1997; Cherniak and Watson, 2000). Pb diffusion in the amorphous phase is also faster than Pb diffusion in zircon that was implanted by Pb ions, which caused artificial radiation damage and probably enhanced the Pb mobility (Cherniak et al., 1991). It is difficult to verify the validity of our estimated diffusion coefficients since—as far as we know—they are the first experimental estimates for diffusion of these species in the amorphous zircon phase. However, evidence for the validity of our model assumptions is that the degree of radionuclide loss is the same in both experiments despite the obvious differences in the kinetics of rim formation (Fig. 1) and the nature and strength of ion exchange (Fig. 2).

3.3. Implications for zircon geochronology and for the application of zircon as a nuclear waste form

Before we assess the implication of our diffusion coefficients for zircon geochronology and nuclear waste immobilization in zircon, we would like to point out that our diffusion coefficient are more likely underestimated than overestimated because leaching reactions might have created a narrower net of fast diffusion pathways within the leached areas, i.e., r in Eq. (1) is smaller than assumed. Furthermore, if one assumes that diffusion occurs uniformly throughout the metamict zircon, i.e., neglecting the occurrence of fast diffusion channels, the diffusion coefficients would be several orders of magnitude higher since diffusion occurred over a length scale of several micrometers during the relative short period of the experiment.

Based on the estimated diffusion coefficients, we can calculate from Eq. (1) that a completely amorphous zircon with a typical radius of 50 μm held at a temperature of 175 °C will have lost more than ~ 2% of its radiogenic Pb and about 2% of U after 10^4 years, and more than ~ 23% and about 20%, respectively, after 10^6 years. We should emphasize, however, that these calculations only take into account volume diffusion through uniformly amorphous zircon and ignore any enhancement of the effective diffusion by high diffusivity domain boundaries. Our results thus provide the first evidence for an old proposal (e.g., Nicolaysen, 1957; Tilton, 1960) that recent Pb loss discordias could be the direct result of Pb loss by volume diffusion. Nevertheless, two important requirements constrain this assumption: (1) the zircon has to be heavily metamict (i.e., it should fit at least above the first percolation point), and (2) it has to remain for a sufficiently long time at moderate temperatures where recrystallization of amorphous zircon is not significant within geological time scales (i.e., below ~500 °C under dry conditions; Geisler et al., 2001a). Unfortunately, U–Pb investigations of zircon are rarely accompanied by complementary chemical analyses to conclude about the Pb loss mechanism. However, we found one example where Pb loss by volume diffusion could clarify otherwise unexplained discordant U–Pb ages: SHRIMP analyses from a 4.4-Ga old, metamict (α-decay dose up to ~ 21×10^{18} α-decays/g) zircon grain from the Jacks Hills conglomerate in Western Australia define a linear discordance pattern that points to the origin of the Concordia, clearly indicating recent Pb loss (Wilde et al., 2001). Selective Pb loss through leaching by a meteoric fluid is highly unlikely in this case because (a) high δ^{18}O values as measured by ion microprobe do not indicate

an exchange with low $\delta^{18}O$ meteoric water (however, isotope re-equilibration by enhanced oxygen diffusion in the metamict network cannot be excluded), (b) electron microprobe measurements obviously did not reveal high concentrations of non-formula element such as Ca and Al, and (c) the REE patterns from this zircon resemble those known from other natural, unaltered zircons (see Wilde et al., 2001).

The combination of reaction structures, elemental diffusion and structural recovery observed in the present study under a rather low temperature provides important constraints for the interpretation of zircon structures and U–Pb discordance observed in natural zircon systems. For example, Högdahl et al. (2001) interpreted the U–Pb discordance detected in milky-white zircons of a mylonitic gneiss from the Fennoscandian Shield in central Sweden to be the result of low temperature (150–200 °C) hydrothermal alteration, which obviously also causes some structural recovery as seen by Raman spectroscopy. Another example is a natural metamict zircon from Ontario, Canada, that exhibits a network-like alteration pattern similar to that of grains treated with HCl–$CaCl_2$ (Fig. 1D–F) (Lumpkin, 2001), again pointing to the importance of our experimental findings for the interpretation of alteration patterns in natural zircons. Additionally, rim–core structures such as those shown in Fig. 1A–C have also been reported from zircons from a large number of high-grade metamorphic rocks, as discussed in more detail by Geisler et al. (2001b).

With respect to the safe storage of plutonium in zircons, our experimental results clearly demonstrate that fluid temperatures of less than 200 °C can cause significant alteration (including fracturing) of radiation-damaged zircon, which should be seriously considered when evaluating the application of zircon as a host phase for Pu waste immobilization. The proposed transport model suggest that the long-term stability of a zircon waste form against natural fluids strongly depends on the waste loading, which determines the degree of accumulated damage with storage time. However, our diffusion coefficients suggest that mobilization of hazardous actinides from a completely amorphous zircon waste form by simple volume diffusion is limited as long as the surface area to volume ratio is large, as would be the case for non-fractured pellets or monolithic blocks.

4. Summary and conclusion

It has been shown that the fast transport of chemical species from and into the metamict network can be well explained by the microstructure of a partially metamict zircon, i.e., by the existence of percolating domain boundaries or areas of low atomic density, which act as fast diffusion pathways. According to the proposed percolation-type model for diffusion, the effective diffusion of any species within the zircon lattice should vary with the α-decay dose, i.e., the degree of metamictization. The proposed percolation-type diffusion model provides for the first time a physical explanation for the relationship between the degree of metamictization and age discordance as observed by SHRIMP and Micro-Raman measurements (Nasdala et al., 1998), and more generally for the correlation between the U content and age discordance in zircon often reported in U–Pb zircon studies (e.g., Silver and Deutsch, 1963). In addition, the stability of U and the higher degree of structural recovery observed in hydrothermal experiments, which were performed at higher temperatures (Geisler et al., 2001b), indicate that the dynamics of structural rearrangements of metamict zircon during fluid–zircon interaction play an important role in controlling the leaching process, and especially the loss of U and Th. The difference of the kinetics of rim formation in both experiments is evidence that the leaching kinetics (i.e., rim formation) is not only controlled by structural properties but also by the composition and the pH of the solution, which has yet to be investigated in more detail. Although both solutions have no direct natural analogs and thus our experimental results cannot directly be transferred to natural conditions, they suggest that within geological time scales, leaching of metamict zircon through natural waters can be significant even at temperatures below 200 °C, as indicated by studies on natural zircons (e.g., Högdahl et al., 2001; Lumpkin, 2001). This is further supported by reports of natural Ca- and Al-rich metamict zircons (e.g., Speer, 1980; Geisler and Schleicher, 2000), some of which unambiguously have not suffered any high temperature metamorphic imprint (Geisler and Schleicher, 2000). Our results also suggest that volume diffusion of Pb in metamict zircon has to be taken into account seriously as a possibility when interpreting recent Pb loss discordias although a fluid

is much more effective in resetting or disturbing the isotopic system of a metamict zircon. Finally, we would like to note that our percolation-type diffusion model might also explain alteration features of other metamict minerals (see Lumpkin, 2001), which should be kept in mind when investigating their suitability as actinide-doped waste forms.

Acknowledgements

We acknowledge the technical assistance of A. Kennedy and A.A. Nemchin (SHRIMP), B. Cornelisen (EMP), P. Chapman (Raman spectroscopy), and B. Mihailova (IR spectroscopy). Many thanks go to J.K.W. Lee, W.T. Lee, E.K.H. Salje, C. Vellmer, and M. Zhang for reviewing an early draft of the manuscript. We would like to thank I.S. Williams and an anonymous reviewer for their constructive comments. TG was supported by grants GE 1094/1-1 and GE 1094/1-2 from the Deutsche Forschungsgemeinschaft (DFG). **[EO]**

References

Bischoff, J.L., Rosenbauer, R.J., Fournier, R.O., 1996. The generation of HCl in the system $CaCl_2$-H_2O: vapor-liquid relations from 380–500 °C. Geochim. Chosmochim. Acta 60, 7–16.

Black, L.P., 1987. Recent Pb loss in natural zircon: a natural or laboratory-induced phenomenon? Chem. Geol. 65, 25–33.

Bogomolov, Y.S., 1991. Migration of lead in non-metamict zircon. Earth Planet. Sci. Lett. 107, 625–633.

Brookins, D.G., 1984. Geochemical Aspects of Radioactive Waste Disposal Springer Verlag, New York.

Capitani, G.C., Leroux, H., Doukhan, J.C., Ríos, S., Zhang, M., Salje, E.K.H., 2000. A TEM investigation of natural metamict zircons: structure and recovery of amorphous domains. Phys. Chem. Miner. 27, 545–556.

Chakoumakos, B.C., Murakami, T., Lumkin, G.R., Ewing, R.C., 1987. Alpha-decay-induced fracturing in zircon: the transition from the crystalline to the metamict state. Science 236, 1556–1559.

Cherniak, D.J., Watson, E.B., 2001. Pb diffusion in zircon. Chem. Geol. 172, 5–24.

Cherniak, D.J., Lanford, W.A., Ryerson, F.J., 1991. Lead diffusion in apatite and zirconusing ion implantation and Rutherford backscattering techniques. Geochim. Cosmochim., 1663–1673.

Cherniak, D.J., Hanchar, J.M., Watson, E.B., 1997a. Rare-earth diffusion in zircon. Chem. Geol. 134, 289–301.

Cherniak, D.J., Hanchar, J.M., Watson, E.B., 1997b. Diffusion of tetravalent cations in zircon. Contrib. Mineral. Petrol. 127, 383–390.

Claoué-Long, J.C., Compston, W., Roberts, J., Fanning, C.M., 1995. Two Carboniferous ages: a comparison of SHRIMP zircon dating with conventional zircon ages and $^{40}Ar/^{39}Ar$ analyses: geochronology, time scales and global stratigraphic correlation. Soc. Sediment. Geol. Spec. Publ. 54, 3–21.

Crocombette, J.-P., Ghaleb, D., 2001. Molecular dynamics modeling of irradiation damage in pure and uranium-doped zircon. J. Nucl. Mater. 295, 167–178.

Davis, D.W., Krogh, T.E., 2000. Preferential dissolution of ^{234}U and radiogenic Pb from a-recoil-damaged lattice sites in zircon: implications for thermal histories and Pb isotopic fractionation in the near surface environment. Chem. Geol. 172, 41–58.

DeLaeter, J.R., Kennedy, A.K., 1998. A double focussing mass spectrometer for geochronology. Int. J. Mass Spectrom. Ion Process. 178, 43–50.

Ewing, R.C., 1999. Nuclear waste forms for actinides. Proc. Natl. Acad. Sci. U. S. A. 96, 3432–3439.

Ewing, R.C., Haker, R.F., Lutze, W., 1982. Leachability as a function of alpha dose. In: Lutze, W. (Ed.), Scientific Basis for Nuclear Waste Management V, North Holland, New York, pp. 387–389.

Ewing, R.C., Lutze, W., Weber, W.J., 1995. Zircon: a host phase for the disposal of weapons plutonium. J. Mater. Res. 10, 243–246.

Farnan, I., Salje, E.K.H., 2001. The degree and nature of radiation damage in zircon observed by ^{29}Si nuclear magnetic resonance. J. Appl. Phys. 89, 2084–2090.

Frape, S.K., Fritz, P., 1987. Geochemical trends for groundwaters from the Canadian Shield. Saline Water and Gasses in Crystalline Rocks. Geol. Assoc. Canada Spec. Pap., vol. 33, pp. 19–38.

Geisler, T., Pidgeon, R.T., 2001. Significance of radiation damage on the integral SEM cathodoluminescence intensity of zircon: an experimental annealing study. N. Jb. Miner. Mh. 10, 433–445.

Geisler, T., Schleicher, H., 2000. Improved U–Th–total Pb dating of zircons by electron microprobe using a new background modeling method and Ca as a chemical indicator of fluid-induced U–Th–Pb discordance in zircon. Chem. Geol. 163, 269–285.

Geisler, T., Pidgeon, R.T., van Bronswijk, W., Pleysier, R., 2001a. Kinetics of thermal recovery and recrystallization of partially metamict zircon: a Raman spectroscopic study. Eur. J. Mineral. 13, 1163–1176.

Geisler, T., Ulonska, M., Schleicher, H., Pidgeon, R.T., van Bronswijk, W., 2001b. Leaching and differential recrystallization of metamict zircon under experimental hydrothermal conditions. Contrib. Mineral. Petrol. 141, 53–65.

Hansen, B.T., Friderichsen, J.D., 1989. The influence of recent lead loss on the interpretation of disturbed U–Pb systems in zircons from igneous rocks in East Greenland. Lithos 3, 209–223.

Högdahl, K., Gromet, L.P., Broman, C., 2001. Low P–T Caledonian resetting of U-rich Paleoproterozoic zircons, central Sweden. Am. Mineral. 86, 534–546.

Krogh, T.E., Davis, G.L., 1975. Alteration in zircons and differential dissolution of altered and metamict zircon. Carnegie Inst. Wash., Year Book 74, 619–623.

Lee, J.K.W., Tromp, J., 1995. Self-induced fracture generation in zircon. J. Geophys. Res. 100 (B9), 17750–17753.

Lee, J.K.W., Williams, I.S., Ellis, D.J., 1997. Pb, U and Th diffusion in natural zircon. Nature 390, 159–162.

Lumpkin, G.R., 2001. Alpha-decay damage and aqueous durability of actinide host phases in natural systems. J. Nucl. Mater. 289, 136–166.

McLaren, A.C., Fitz Gerald, J.D., Williams, I.S., 1994. The microstructure of zircon and its influence on the age determination from U/Pb isotopic ratios measured by ion microprobe. Geochim. Cosmochim. Acta 58, 993–1005.

Murakami, T., Chakoumakos, B.C., Ewing, R.C., Lumpkin, G.R., Weber, R.W.J., 1991. Alpha-decay event damage in zircon. Am. Mineral. 76, 1510–1532.

Nasdala, L., Pidgeon, R.T., Wolf, D., Irmer, G., 1998. Metamictization and U–Pb isotopic discordance in single zircons: a combined Raman microprobe and SHRIMP ion probe study. Mineral. Petrol. 62, 1–27.

Nelson, D.R., 1997. Compilation of SHRIMP U–Pb zircon geochronology data, 1996. Geol. Surv. West. Aust., Rec. 1997/2 198 pp.

Nicolaysen, L.O., 1957. Solid diffusion in radioactive minerals and the measurement of absolute age. Geochim. Cosmochim. Acta 11, 41–59.

Pekdeger, A., Jarmersted, C.S., Thomas, L., 1994. Hydrochemical sampling of formation waters at the KTB-borehole and their chemical composition. Sci. Drill. 4, 101–111.

Petit, J.C., Ran, J.C., Paccagnella, A., 1989. Structural dependence of crystalline silicate hydration during aqueous dissolution. Earth Planet. Sci. Lett. 93, 292–296.

Pidgeon, R.T., O'Neil, J.R., Silver, R.T., 1966. Uranium and lead isotopic stability in a metamict zircon under experimental hydrothermal conditions. Science 154, 1538–1540.

Pidgeon, R.T., O'Neil, J.R., Silver, R.T., 1973. Observations on the crystallinity and the U–Pb system of a metamict Ceylon zircon under experimental hydrothermal conditions. Fortschr. Mineral. 50, 118.

Pidgeon, R.T., O'Neil, J.R., Silver, R.T., 1995. The interdependence of U–Pb stability, crystallinity and external conditions in natural zircons—an early experimental study. Leon T Silver 70th Birthday Symposium and Celebration. California Institute of Technology, pp. 225–231, Extended Abstracts.

Reichenberg, D., 1953. Properties of ion-exchange resins in relation to their structure: III. Kinetics of exchange. J. Am. Chem. Soc. 75, 589–597.

Ríos, S., in preparation. Conventional X-rays for characterization of amorphous phases. Phase Transit. (submitted for publication).

Ríos, S., Salje, E.K.H., Zhang, M., Ewing, R.C., 2000. Amorphization in zircon: evidence for direct impact damage. J. Phys., Condens. Matter 12, 2401–2412.

Rizvanova, N.G., Levchenkov, O.A., Belous, A.E., Bezmen, N.I., Maslenikov, A.N., Komarov, A.N., Makeev, A.F., Levskii, L.K., 2000. Zircon reaction and stability of the U–Pb isotope system during interaction with carbonate fluid: experimental hydrothermal study. Contrib. Mineral. Petrol. 139, 101–114.

Salje, E.K.H., Chrosch, J., Ewing, R.C., 1999. Is "metamictization" of zircon a phase transition? Am. Mineral. 84, 1107–1116.

Silver, L.T., Deutsch, S., 1963. Uranium–lead isotopic variations in zircon: a case study. J. Geol. 71, 721–758.

Sinha, A.K., Wayne, D.M, Hewitt, D.A., 1992. The hydrothermal stability of zircon: preliminary experimental and isotopic studies. Geochim. Cosmochim. Acta 56, 3535–3551.

Speer, J.A., 1980. Zircon. In: Ribbe, P.H. (Ed.), Reviews in Mineralogy 5Mineral. Soc. Am., pp. 76–122.

Stern, T.W., Goldich, S.S., Newell, M.F., 1966. Effects of weathering on the U–Pb ages of zircon from the Morton Gneiss, Minnesota. Earth Planet. Sci. Lett. 1, 369–371.

Tilton, G.R., 1960. Volume diffusion as a mechanism of discordant lead ages. J. Geophys. Res. 65, 2933–2945.

Tole, M.P., 1985. The kinetics of dissolution of zircon ($ZrSiO_4$). Geochim. Cosmochim. Acta 49, 453–458.

Trachenko, K., Dove, M.T., Salje, E.K.H., 2000. Modeling the percolation-type transition in radiation damage. J. Appl. Phys. 87, 7702–7707.

Trachenko, K., Dove, M.T., Salje, E.K.H., 2001. Atomistic modeling of radiation damage in zircon. J. Phys., Condens. Matter 13, 1947–1959.

Trocellier, P., Delmas, R., 2001. Chemical durability of zircon. Nucl. Instrum. Methods Phys. Res., B 181, 408–412.

Weber, W.J., Ewing, R.C., Wang, L.-M., 1994. The radiation-induced crystalline-to-amorphous transition in zircon. J. Mater. Res. 9, 688–698.

White, D.E., 1965. Saline waters off sedimentary rocks. In: Fluids in subsurface environments—a symposium. Am. Assoc. Pet. Geol. Mem. 4, 342–366.

Wilde, S.A., Valley, J.W., Peck, W.H., Grahams, C.M., 2001. Evidence from detrital zircons from the existence of continental crust and oceans on the Earth 4.4Gyr ago. Nature 409, 175–178.

Zhang, M., Salje, E.K.H., 2001. Infrared spectroscopic analysis of zircon: Radiation damage and the metamict state. J. Phys., Condens. Matter 13, 3057–3071.